Interactions between Methacrylic Acid/Ethyl Acrylate Copolymers and Dodecyltrimethylammonium Bromide

C. Wang and K. C. Tam*

School of Mechanical and Production Engineering, Nanyang Technological University, 50 Nanyang Avenue, Singapore 639798, Republic of Singapore

R. D. Jenkins and C. B. Tan

The Dow Chemical Company, Asia-Pacific Technical Center, 16 Science Park Drive, Singapore 118227, Republic of Singapore

Received: May 25, 2002; In Final Form: February 22, 2003

The interactions between dodecyltrimethylammonium bromide (DoTab) and methacrylic acid/ethyl acrylate copolymers were studied using isothermal titration calorimetry (ITC) and laser light scattering (LLS) techniques. Individual cationic surfactant molecules first bind to negatively charged carboxylate groups on the polymer chains due to electrostatic attraction. In this regime, a pronounced endothermic peak is detected in the enthalpy curve and a slight reduction in the particle size is observed. When C' (indicated by another endothermic peak) is reached, the micellization of electrostatically bound surfactant commences and the particle size increases by several orders of magnitude. It then precipitates, producing a large hydrophobic polymer/surfactant complex. With further addition of surfactant, free micelles begin to form, and the precipitates resolublize (for the polymers with lower charge density) or gelatinize (for the polymers with higher charge density). The thermodynamic parameters derived from ITC measurements suggest that the electrostatic binding is an endothermic process driven by entropy. The positive entropy is attributed to the recovery of translational entropy of released counterions from bound surfactant molecules. Addition of salt screens the electrostatic repulsion between surfactant headgroups and attraction between oppositely charged polymer chains and surfactant molecules, which weakens the binding of surfactant onto the polymers favoring the formation of free micelles.

Introduction

Interactions between polymers and surfactants bearing opposite charges have attracted increasing attention because of their interesting and complex behaviors. These systems have widespread applications in rheological control, detergency, pharmaceuticals, etc.[1−11] The interactions between oppositely charged polymers and surfactants are usually stronger because of the Coulombic attractive force. Such binding commences at surfactant concentration several magnitudes lower than the critical micelle concentration (cmc). The binding can be considered as an ion-exchange process, in which condensed counterions on the polymer chains are replaced by bound surfactant molecules.[5,8−12] Typically, the electrostatic binding is reinforced by either the micellization of polymer-bound surfactant or the cooperative aggregation between the alkyl chains of bound surfactant and hydrophobic segment of polymer chains.[8−12] Numerous research groups have sought to advance the fundamental understanding on the thermodynamics governing the processes of binding, micellization, and aggregation using a variety of experimental techniques such as surface tension measurement,[4] potentiometry,[1] electromotive force (EMF) measurement,[1−3] light scattering,[6,11] fluorescence quenching,[11,13] and microcalorimetry.[2,3,7,9,10,14−20] A modern calorimetric technique such as isothermal titration calorimetry (ITC) is one of the most sensitive techniques that permits the direct measurement of thermodynamic changes during the course of binding and micellization. Thermodynamic parameters such as enthalpy (ΔH), entropy (ΔS), Gibbs energy (ΔG), and heat capacity (C_p), which are crucial to the understanding and theoretical description of polymer/surfactant interactions, can be extracted from the ITC binding profiles.[2,3,7,9,10,14−20] From the thermodynamic parametrization and theoretical modeling using Manning's counterion condensation theory, it was observed that the electrostatic binding is entropy-driven and enthalpy-opposed and controlled by the linear charge spacing on the polymer chain and the ionic strength of the solution.[8−10] Microcalorimetry also allows the characterization of polymer/surfactant system in terms of critical concentrations, such as critical aggregation concentration (cac) corresponding to the onset of binding, saturation concentration (C_2) corresponding to the saturation of polymer chains with bound surfactant, and the second critical concentration (C_m) corresponding to the formation of free micelles in the polymer solution.

It has been reported that ionic surfactant molecules bind to oppositely charged sites on polymer chains in stoichiometric proportions.[10,12,21] A typical example is the binding of sodium dodecyl sulfate (SDS) to protein molecules, which has been extensively studied since the 1930s.[12,21] An interesting phenomenon noted by many researchers is that the polymer/surfactant complex precipitates from aqueous solution when the amount of positive and negative charges are equivalent, whereas such precipitates can be resolublized in excess amounts of surfactant.[12,22] Ohbu et al. revealed some important features on

* To whom correspondence should be addressed. Fax: 65-6791-1859. E-mail: mkctam@ntu.edu.sg.

10.1021/jp026184g CCC: $25.00
Published on Web 04/18/2003

the binding of SDS to cationic cellulose using dialysis method. Binding was found to occur at very low SDS concentration, and the degree of binding, β (defined as the molar ratio between the oppositely charged groups from surfactant and polyion) approached 0.5 when the concentration is only 1/20th of the cmc. Precipitates were produced at $\beta = 1$, and the precipitates were resolubilized when β reached 3, which corresponded to the cmc of SDS.[12] Kwak and co-workers have conducted extensive studies on the binding of cationic surfactants to a series of anionic polyelectrolytes. They observed that the binding is highly cooperative; β increases sharply over a narrow surfactant concentration range and levels off at a value less than unity, when the negative charges of the polyanions are saturated.[12,22] The precipitation and resolublization normally involve a substantial change in the polymer conformation, for example, protein undergoes a conformational change from random structure to a folded helix surrounded by surfactant micelles with the addition of SDS.[12,21,22] Goddard et al. presented the multiequilibrium phase diagram determined from surface tension studies, which describes the structure of polycation/anionic surfactant complexes.[12] They hypothesized that the formation of a highly surface-active macromolecular species with extended alkyl groups is responsible for the high surface activity in the precipitation region. The subsequent resolublization of the complex is due to a second layer of bound surfactants with their ionic headgroups pointing outwards which are attached to the first bound layer through the association with the alkyl chains, and this transforms the insoluble polymer/surfactant complex into a soluble polyelectrolyte-like complex.[12] Despite these studies, the nature of the polymer/surfactant complexation is still not resolved, and the mechanisms of precipitation and resolublization and the structure of the polymer/surfactant complex are still subject of continual discussion and debates.

In this study, the interactions between methacrylic acid/ethyl acrylate copolymers and dodecyltrimethylammonium bromide (DoTab) were studied using isothermal titration calorimetry (ITC) and laser light scattering (LLS) techniques. The enthalpy profiles can be characterized in terms of the critical concentrations and thermodynamic parameters by analyzing the isothermal titration data. The mechanism of polymer/surfactant complexation and the microstructure of the polymer/surfactant complex can be elucidated from light scattering. The effect of salt on the binding and micellization behaviors were also examined.

Experimental Details

Materials. The methacrylic acid/ethyl acrylate copolymers examined in this study were synthesized by Dow Chemicals using conventional semicontinuous emulsion polymerization. They have an average molecular weight of approximately 200 000−250 000 Da, as determined from static light scattering measurements.[23,24] These polymers are designated as HASE*x*−*y*, where *x* and *y* correspond to the molar percentage of the methacrylic acid (MAA) and ethyl acrylate (EA) groups, respectively. The cationic surfactants used in the studies of polymer/surfactant interactions are dodecyltrimethylammonium bromide (DoTab from Fluka, ≥98%, $C_{15}H_{34}BrN$), tetradecyltrimethylammonium bromide (TTab, from Tokyo Kasei, ≥99%, $C_{17}H_{34}BrN$), and cetyltrimethylammonium bromide (CTab, from Merck, ≥99%).

Sample Preparation and Measuring Techniques. The polymer latex at low pH (ca 3−4) was dialyzed in distilled−deionized water using regenerated cellulose tubular membrane. The dialysis process was carried out over a 1-month period during which most of the impurities and unreacted chemicals were removed. A 3 wt % stock solution was prepared and stored at 4 °C prior to use. From the stock solution, completely neutralized 0.05 wt % polymer solutions (using 1 M standard NaOH solution from Merck) were prepared for microcalorimetric titration and light scattering studies.

The calorimetric data were obtained using the Microcal isothermal titration calorimeter (ITC). This power compensation, differential instrument was previously described in detail by Wiseman et al.[25,26] It has a reference and a sample cell of approximately 1.35 mL, and the cells are both insulated by an adiabatic shield. The titration was carried out at 25.0 ± 0.02 °C by injecting 0.1 M surfactant solution from a 250 μL injection syringe into the sample cell filled with 0.05 wt % polymer solution. The syringe is tailor-made so that the tip acts as a blade-type stirrer to ensure an optimum mixing efficiency at 400 rpm. An injection schedule was automatically carried out using interactive software after setting up the number of injections, volume of each injection, and time between each injection.

The Brookhaven laser light scattering system was used to determine the hydrodynamic radius (R_h) and radius of gyration (R_g). The equipment consists of a BI200SM goniometer, BI-9000AT digital correlator, and other supporting data acquisition and analysis software and accessories. An argon-ion vertically polarized 488 nm laser was used as the light source. The $G_2(t)$ functions obtained from dynamic light scattering were analyzed using the inverse Laplace transformation technique (regularized positive exponential sum, namely, REPES in our case) to produce the distribution function of decay times. Several measurements were carried out at 90° for a given sample to obtain an average hydrodynamic radius.

Results and Discussion

Overview on the Binding of DoTab to HASE Polymers. The isothermal titration experiments were conducted by step-by-step injections of surfactant solution into the sample cell filled with HASE polymer solutions. Figure 1a shows the thermogram that depicts the raw heat signal (cell feedback, CFB, in μcal/sec) from the gradual injections of 0.1 M DoTab solution into 0.05 wt % HASE70−30 in 0.1 M NaCl solution. Integration of the area under the raw signals, corrected for the heat of dilution obtained from a blank titration, gave the differential enthalpy curves as shown in Figure 1b. However, the enthalpy of dilution is small compared to the micellization and binding processes. The differential enthalpy curves for titrating 0.1 M DoTab into 0.05 wt % HASE polymer solutions in the presence of 0.1 M NaCl are plotted in Figure 2, together with the dilution curve of 0.1 M DoTab into 0.1 M NaCl solution. The differential enthalpy curves for titrating 0.1 M DoTab ($N_{carbon} = 12$), TTab ($N_{carbon} = 14$) and CTab ($N_{carbon} = 16$) solutions into 0.05 wt % HASE70−30 polymer in 0.1 M NaCl solution are shown in Figure 3. As shown in Figures 2 and 3, two endothermic peaks (indicated by "A" and "B") were observed in the early stages of the titration. The onset and position of peak A are independent of the alkyl chain length of the surfactants, and the breadth is proportional to the molar percentage of MAA content. This endothermic peak is believed to represent the electrostatic binding of positively charged surfactant monomers to the anionic carboxylate sites along the polymer chains.[10] The onset of peak B decreases from ~7.36 to 4.04 mM as the carbon numbers of the hydrophobic tail increase from 12 to 16, suggesting that this peak may be attributed to hydrophobic interaction. We have previously observed that the blocky EA segments are sufficiently hydrophobic to induce association between neighboring polymer

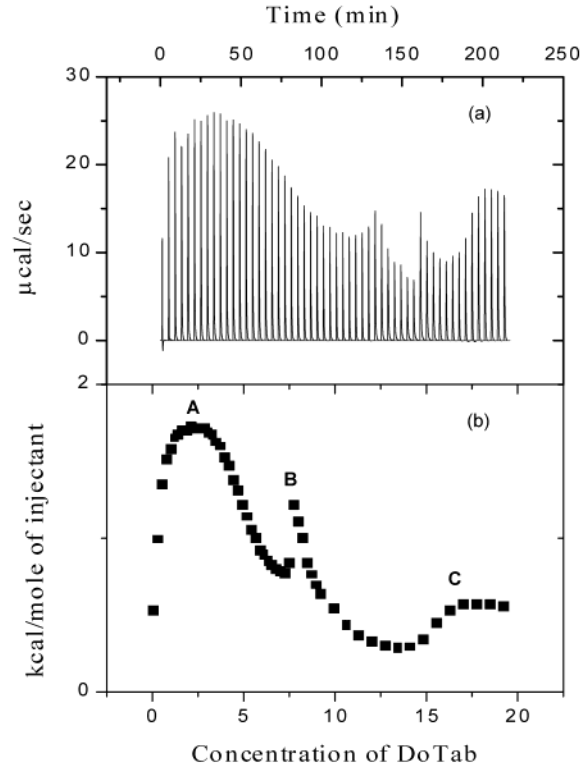

Figure 1. Calorimetric titration of 0.1 M DoTab into 0.05 wt % HASE70−30 in 0.1 M NaCl solution: (a) thermogram showing cell feedback (CFB) versus time; (b) differential enthalpic curves versus the concentration of DoTab.

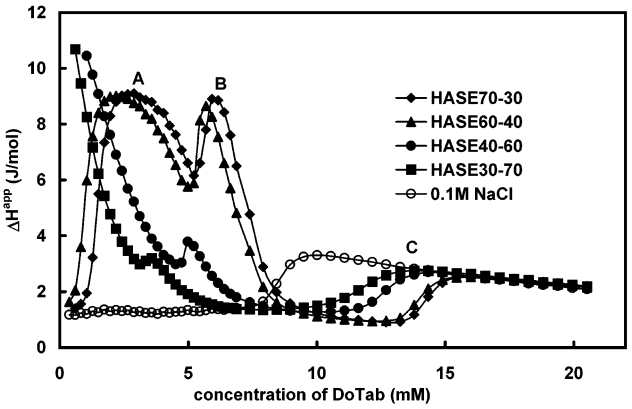

Figure 2. Differential enthalpy curves of titrating 0.1 M DoTab into 0.05 wt % HASE series polymers in 0.1 M NaCl solutions: (◆) HASE70−30; (▲) HASE60−40; (●) HASE40−60; (■) HASE30−70.

chains to produce a swollen cluster of 3−5 chains.[24,27] Thus peak B is believed to characterize the hydrophobic association between the polymer-bound surfactant molecules and EA segments, resulting in the formation of mixed micelles at EA segments. The third peak (indicated by "C"), which has a profile similar to the dilution curve, is attributed to the formation of free DoTab micelles.[10]

The binding profile characterized in terms of the critical concentrations for HASE70−30/DoTab pair is depicted in Figure 4. The binding deviates from the dilution curve at C_{DoTab} = 1 mM (denoted by C_1), which is the critical concentration at which the onset of electrostatic binding commences. The onset of another well-separated peak (denoted by B) appears at C_{DoTab} = 5.2 mM (C'), which corresponds to the critical micellization concentration for the electrostatically bound surfactant molecules. Subsequently, the enthalpy curve

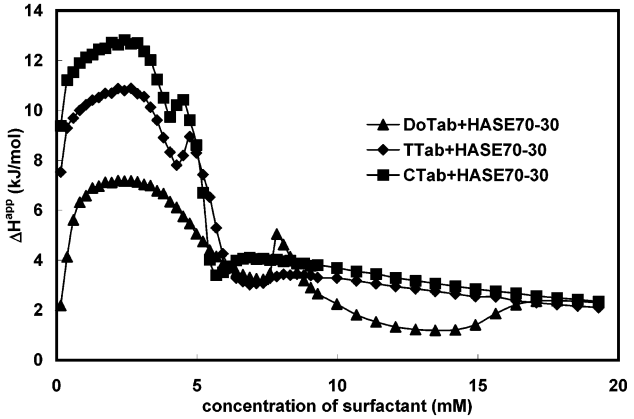

Figure 3. Differential enthalpy curves titrating 0.1 M (▲) DoTab, (◆) TTab, and (■) CTab (■) into 0.05 wt % HASE70−30 in 0.1 M NaCl solution.

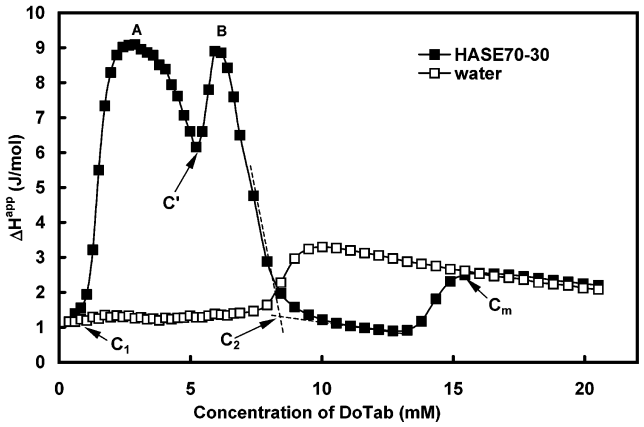

Figure 4. Classification of interaction regimes of HASE/DoTab system: (■) binding curve; (□) dilution curve.

levels off and approaches the dilution curve at C_{DoTab} = 8.5 mM, designated as C_2, which represents the concentration at which the polymer chains are saturated with bound surfactant micelles. With further addition of DoTab, the binding curve merges with the dilution curve at C_{DoTab} = 15 mM, which is designated as C_m corresponding to the formation of free micelles in the polymer solution.

Structural Model of HASE/DoTab Complexation. To identify the microstructure of the polymer/surfactant complex, fully neutralized 0.1 wt % HASE polymer solutions containing different amounts of DoTab were investigated using dynamic and static light scattering techniques. The dependence of scattering intensity on DoTab concentration in the salt-free aqueous solutions of HASE70−30 and HASE30−70 is shown in Figure 5. Figure 6 contains a pictorial description of HASE70−30 polymer solution at different DoTab concentrations, superimposed onto the enthalpy curve determined from ITC measurement. From these two figures, the microscopic binding interaction and macroscopic binding phenomenon can be correlated, and the information extracted from these two figures is summarized as follows. Initially, the polymer solution is transparent, and the scattering intensity is ∼100 kcps in the absence of DoTab. When DoTab was added, the scattering intensity increases gradually until it reaches a threshold, at which the solution turns opaque and the scattering intensity increases sharply by 3 orders of magnitude (>10000 kcps) and the polymer solution precipitates. Comparison drawn from Figures 5 and 6 indicates that the threshold concentration for precipitation agrees with the C' on the ITC profile, suggesting that the

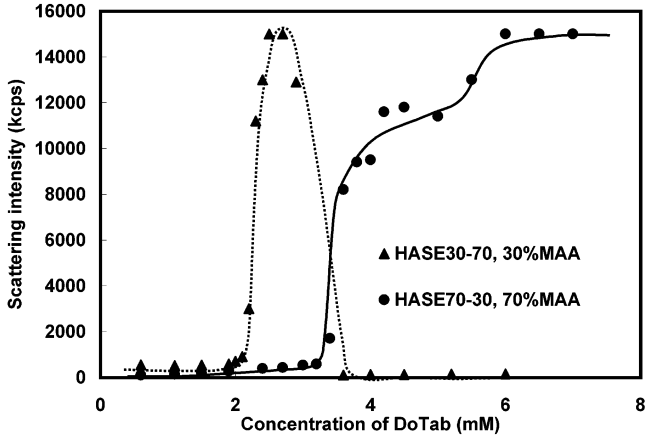

Figure 5. Dependence of scattering intensity on DoTab concentration measured in 0.1 wt % HASE polymer solutions: (▲) HASE30−70; (●) HASE70−30.

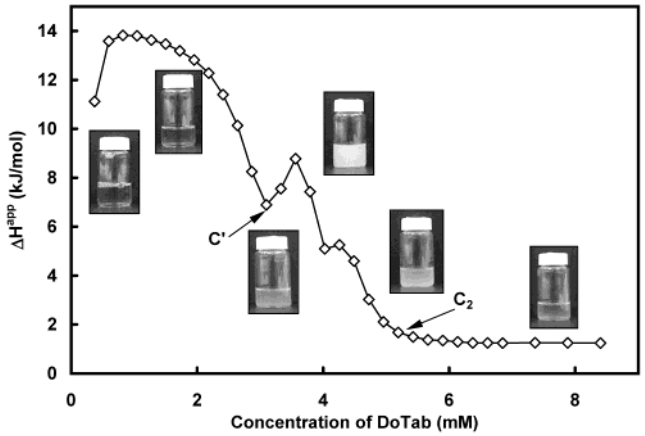

Figure 6. Phase behavior of HASE70−30 at different DoTab concentrations, together with the binding isotherm obtained from ITC.

precipitates from the polymer/surfactant complex are induced by the micellization of polymer-bound DoTab molecules. Moreover, the complexation behavior of HASE/DoTab pair is also dependent on the charge density (MAA/EA molar ratio) of the polymer. For the HASE polymer with low MAA content (e.g., HASE30−70), the precipitation regime is narrow and the polymer/surfactant complex resolublizes with further addition of DoTab, resulting in a sharp decrease in the scattering intensity. However, the precipitates of HASE polymers with high MAA content (e.g., HASE70−30) cannot be resolublized and the scattering intensity remains high. At higher DoTab concentration, the polymer solution becomes very viscous and solid residues adhere to the bottom of the sample bottle, suggesting a gel-like structure is produced.

The relaxation time distribution functions of 0.1 wt % HASE70−30 and HASE30−70 at different DoTab concentrations measured at 90° are shown in Figure 7. The distribution function is broad with relatively low amplitude in the absence of surfactant. When DoTab was added, the relaxation time shifts to lower values, corresponding to a decrease in the size of the aggregate caused by charged shielding from the electrostatically bound DoTab monomers to carboxylate groups. When DoTab concentration reaches a critical value, the relaxation time of the distribution function increases sharply. The width of the peak narrows, and the amplitude become larger. These features are the signature of precipitation of polymer/surfactant complex with a larger particle size. With further addition of DoTab, the mixture either resolublizes (for lower MAA composition) or

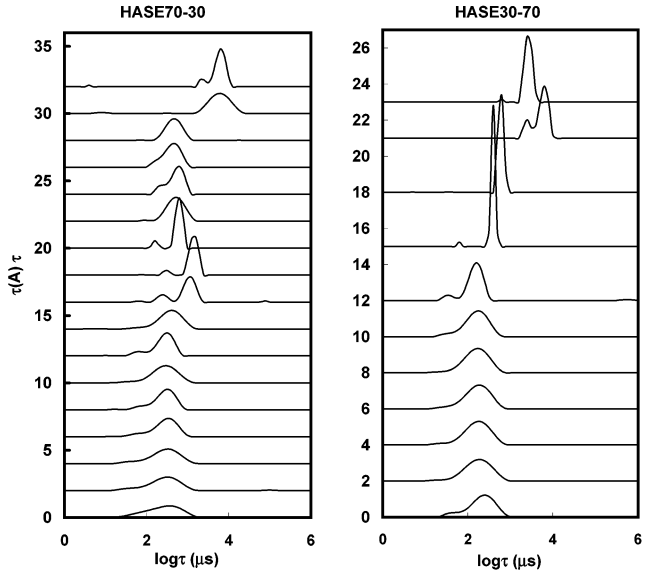

Figure 7. Relaxation time distribution functions of 0.1 wt % HASE70−30 and HASE30−70 solutions at different DoTab concentrations measured at 298 K and 90°.

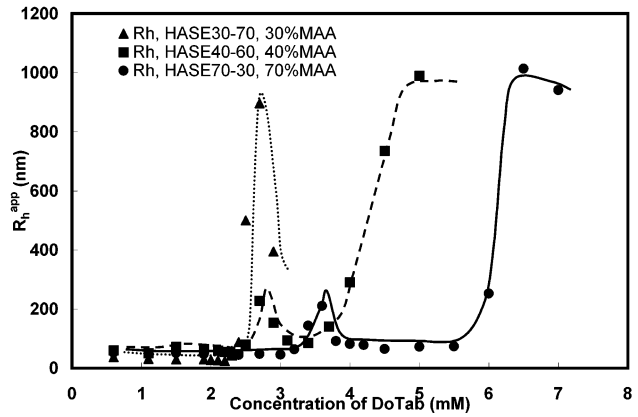

Figure 8. Dependence of R_h^{app} on DoTab concentration in 0.1 wt % HASE solutions: (▲) HASE30−70; (■) HASE40−60; (●) HASE70−30.

gelatinizes (for higher MAA composition), depending on the charge densities of HASE polymers. The apparent hydrodynamic radius (R_h^{app}) can be obtained from the Stokes−Einstein equation:

$$R_h = \frac{kTq^2}{6\pi\eta\Gamma} \tag{1}$$

where k is the Boltzmann constant, q is the scattering vector ($q = 4\pi n \sin(\theta/2)/\lambda$, n is the refractive index of the solution, θ is the scattering angle, and λ is the wavelength of the incident laser light), η is the solvent viscosity, and Γ is the decay rate. Figure 8 shows the R_h^{app} plotted against DoTab concentration for HASE70−30, HASE40−60, and HASE30−70. Initially, R_h^{app} decreases slightly, characterizing the electrostatic binding of DoTab molecules to carboxylate groups on the polymer backbones that shields the electrostatic repulsion between charged polymer chains thereby shrinking the polymer clusters. R_h^{app} then increases sharply and reaches a maximum at a critical DoTab concentration, corresponding to the precipitation of polymer/surfactant complex. It then decreases to a lower equilibrium value. A probable explanation for this is the

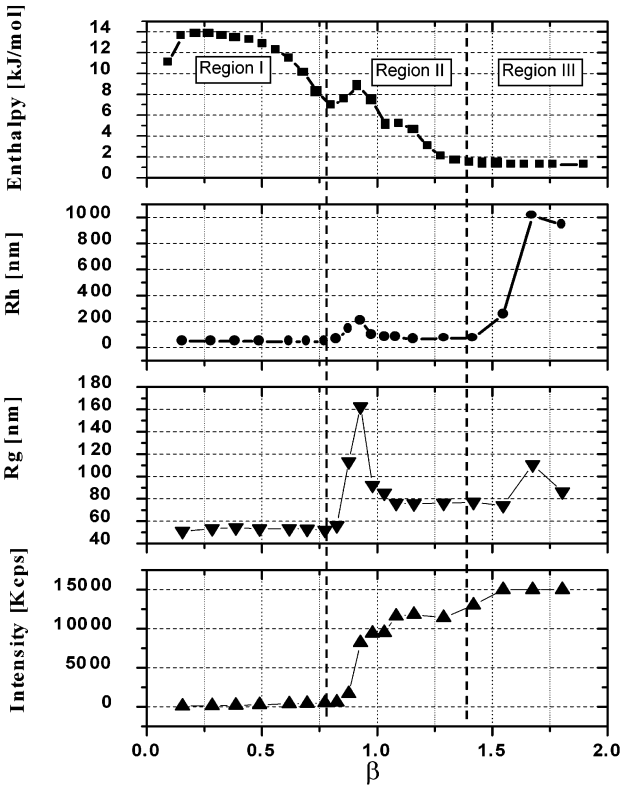

Figure 9. Binding profiles obtained from ITC and light scattering for HASE70−30/DoTab pair.

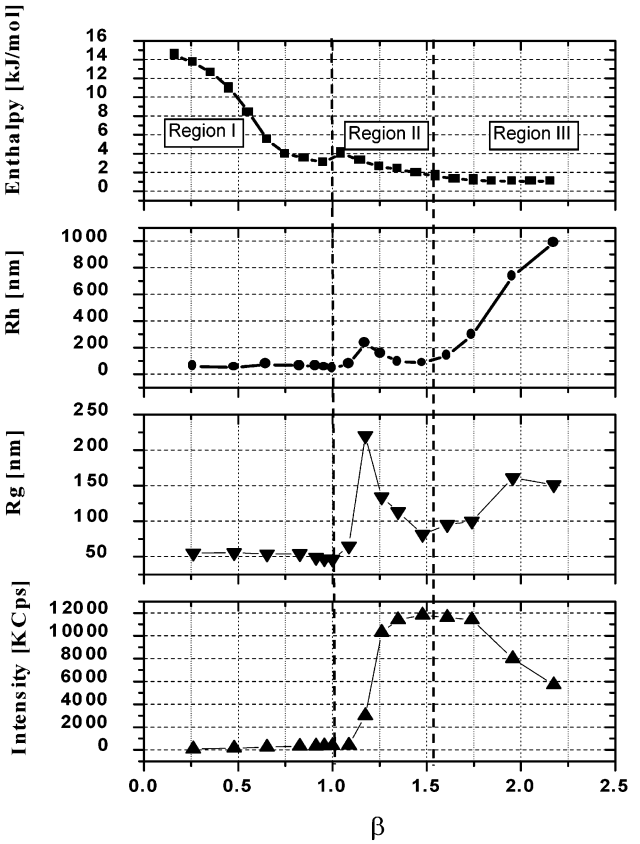

Figure 10. Binding profiles obtained from ITC and light scattering for HASE40−60/DoTab pair.

reorganization of the polymer/surfactant complex structure. For HASE polymer with low MAA content (e.g., HASE30−70), R_h^{app} decreases sharply with DoTab content, characterizing the resolublization of polymer/surfactant complex in excess amount of surfactant. However, for HASE polymer with higher charge density (e.g., HASE70−30), the precipitation of polymer/surfactant complex cannot be resolublized, but it gelatinizes at high DoTab concentration, resulting in an extremely large R_h^{app} that cannot be accurately measured.

The enthalpy curve, radius of gyration (R_g^{app}), hydrodynamic radius (R_h^{app}), and scattering intensity of HASE70−30 and HASE40−60 are plotted together against the charge ratio $\beta = C_{DoTab}/C_{RCOO^-}$ (where C_{DoTab} and C_{RCOO^-} are the molar concentrations of the surfactant and carboxylate groups in solution) in Figures 9 and 10, respectively. At $\beta = 1$, all of the charge sites along the polymer chains are completely bound by the surfactant.

As demonstrated in Figures 9 and 10, the critical concentrations detected from ITC and light scattering are identical. Region I, as characterized by the first endothermic peak, is identified by the slightly decreasing trend of R_h and R_g and the increasing trend of scattering intensity in the same range of β. In this region, the headgroups of DoTab bind to carboxylate groups of HASE polymer to form dodecyltrimethylammonium/carboxylate ion pair ($D^+/\sim COO^-$), which reduces the net charge and weakens the electrostatic repulsion between the polymer chains. Hence, the polymer clusters shrink, resulting in the small decrease in R_h and R_g. In addition, the bound surfactant increases the molar mass of polymer cluster and also strengthens its hydrophobicity, which leads to the slight increase in the scattering intensity. The binding then enters region II when the surfactant concentration reaches C', denoted by the occurrence of the second endothermic peak. In this region, R_h and R_g increase for HASE70−30/DoTab and HASE40−60/DoTab systems from ∼40 to ∼220 nm and from ∼52 to ∼200 nm, respectively, the scattering intensity exhibits a sharp increase by several magnitudes, and the solutions become opaque, characterizing the precipitation of polymer/surfactant complexes. The polymer/surfactant complexation is induced by the micellization of electrostatically bound surfactant molecules at the EA segments of the polymer chains. As suggested by the light scattering data, the micellization is believed to occur between polymer clusters instead of within the polymer clusters because both R_g and R_h exhibit an increase. As shown in Figure 9, R_h^{app} and R_g^{app} decrease from ∼220 to ∼90 nm and from ∼200 to ∼80 nm, respectively, as more DoTab was added. In this regime, the scattering intensity continues to increase with the system remaining opaque. This decrease of particle size may be attributed to the rearrangement of the micellar structure. It is not possible to determine the precise interior structure of the micelle by light scattering techniques alone. It is probable that the micelle self-reorganizes from lamellar stack or cylindrical to a spherical structure, in which the polymer chains are stabilized on the surface of the micelle and the size of the polymer/surfactant complex is reduced (Figure 11b). After the rearrangement, the structure of the complex can be depicted as the "necklace" model, in which the DoTab micelles are denoted as "beads" and polymer chains can be imagined as "strings" attached on the "beads". With further increase in DoTab content, the binding enters region III, where additional surfactant simply increases the number of micelles. Therefore more micelles are present to stabilize the polymer chains, which solublizes the complex (Figure 11d). As shown in Figures 5 and 8, when the $C_{DoTab} > \sim 3$mM, the particle size and scattering intensity decrease and the system becomes completely transparent as the precipitate is resolublized by further addition of DoTab.

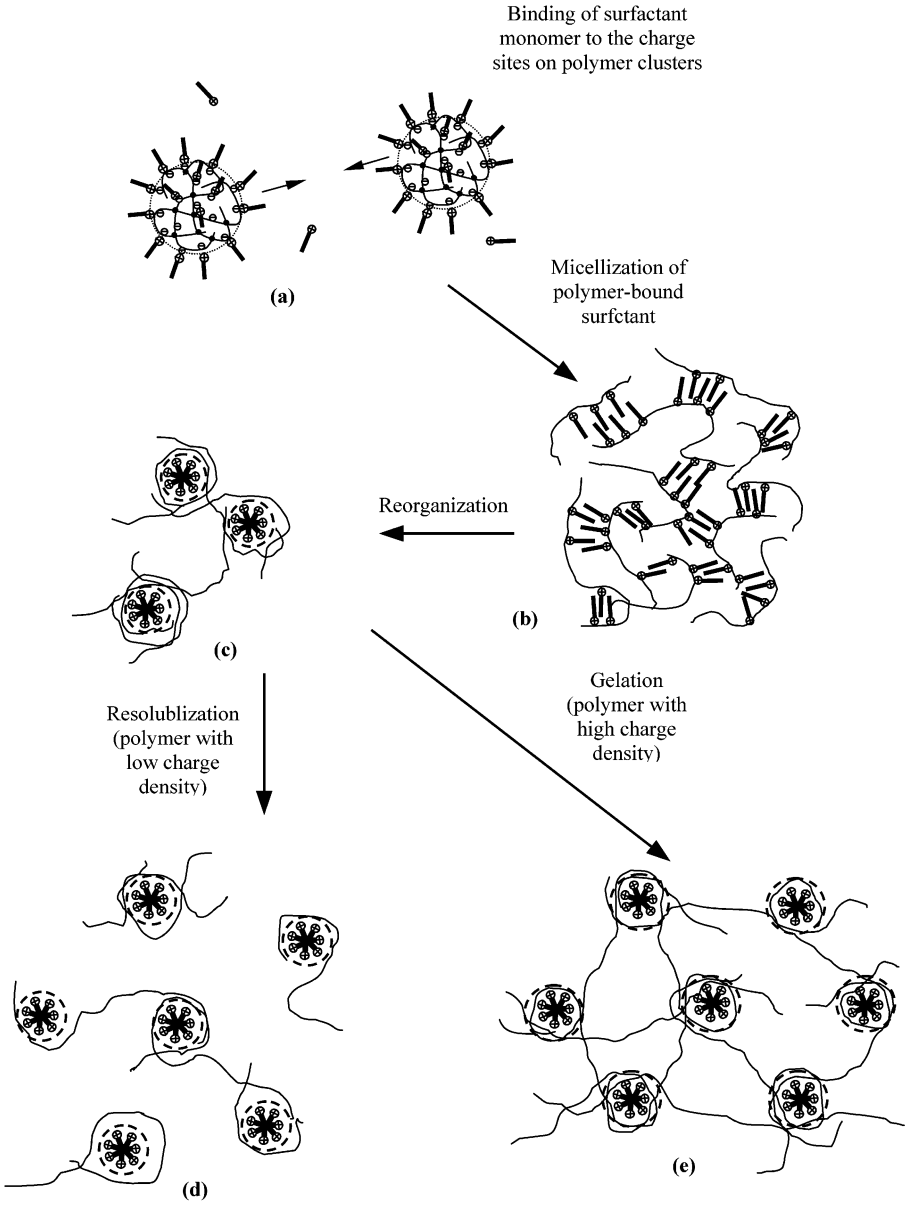

Figure 11. Illustration of binding mechanism and polymer/surfactant complex structure for HASE/DoTab system.

However, the complex is gelatinized instead of resolubilized if the charge density of the polymer is sufficiently high. For the HASE polymer with high MAA content (i.e., HASE70−30), one polymer chain may bind on several micelles simultaneously, through which the polymer chains are physically cross-linked with each other by surfactant micelles to form a network structure (Figure 11e). A complete pictorial representation of binding mechanism and structure of HASE/DoTab complex is given in Figure 11.

Thermodynamic Characterization of Polymer/Surfactant Interactions. As suggested by the binding profiles shown in Figure 2, the electrostatic binding is an endothermic process driven by entropy. The positive entropy gain is attributed to the release of condensed counterions by the bound surfactant. It is known that counterions, that is, Na^+, are condensed on the oppositely charged HASE polymer chains, thereby losing their translational entropy.[10,28] When cationic DoTab was added to the solution of anionic HASE polymer, the electrostatic binding, which can be considered as an ion-exchange interaction, takes place. The condensed sodium ions are released, recovering their translational entropy, which is the essential driving force for the binding to proceed. The thermodynamics of electrostatic binding can be treated by applying Manning's theory of counterion condensation.[28] The binding interaction between DoTab (represented by D^+) and HASE polymer ($\sim COO^-Na^+_m$) can be described by the reaction

$$\sim COO^-Na^+_m + D^+ \leftrightharpoons \sim COO^-D^+ + mNa^+$$

The thermodynamic equilibrium constant, K_T, is given by

$$K_T = \frac{[\sim COO^-D^+][Na^+]^m}{[\sim COO^-Na^+_m][D^+]} \qquad (2)$$

where $[\sim COO^-Na^+_m]$ is the concentration of carboxylate groups with condensed sodium ions, $[\sim COO^-D^+]$ is the concentration of HASE/DoTab complex formed because of electrostatic attractive force, $[D^+]$ is the concentration of unbound DoTab molecules, $[Na^+]$ is the concentration of free sodium ions, and the stoichiometric coefficient m represents the fraction of sodium ions that are thermodynamically condensed on the polymer

TABLE 1: Thermodynamic Parameters Derived from ITC of 0.1 M DoTab into 0.05 wt % HASE series polymers in 0.1 M NaCl

polymer	ΔH_{el} (kJ/mol)	ΔS_{el} (J/(mol K))	ΔG_{el} (kJ/mol)	$\Delta H'$ (kJ/mol)	$\Delta S'$ (J/(mol K))	$\Delta G'$ (kJ/mol)	ΔH_m (kJ/mol)	ΔS_m (J/(mol K))	ΔG_m (kJ/mol)
HASE70−30	9.07	44.83	−4.29	8.90	107.2	−23.05	2.32	69.2	−18.29
HASE60−40	9.10	43.36	−3.82	8.65	107.0	−23.25	2.42	70.0	−18.45
HASE40−60	10.44	45.74	−3.19	3.79	92.2	−23.69	2.60	71.8	−18.79
HASE30−70	10.69	43.93	−2.40	3.20	95.7	−25.32	2.65	73.2	−19.15

chains. The electrostatic binding fraction of the thermodynamic equilibrium constant has the following form:

$$K_b = \frac{[\sim COO^- D^+]}{[\sim COO^- Na^+_m][D^+]} = \frac{K_T}{[Na^+]^m} \quad (3)$$

The thermodynamic equilibrium is reached when the binding of surfactant and release of counterions is in equilibrium, at $K_T = 1$ and $K_b = 1/[Na^+]^m$. According to Manning's theory, m is a function of the reduced linear charge density of polyelectrolyte, ξ:

$$m = 1 - \frac{1}{2\xi} \quad (4)$$

where ξ is related to the Bjerrum length, l_B, and the linear charge spacing of HASE polymer, b,

$$\xi = \frac{l_B}{b} \quad (5)$$

The Bjerrum length is defined as

$$l_B = \frac{e^2}{\epsilon k_B T} \quad (6)$$

where ϵ is the dielectric constant of water, k_B is the Boltzmann constant, and T is the temperature. Thus the electrostatic Gibbs energy change of the binding can be expressed as

$$\Delta G_{el} = -RT \ln K_b = -RT \ln \frac{1}{[Na^+]^m} = mRT \ln [Na^+] \quad (7)$$

The enthalpy for electrostatic binding, ΔH_{el}, is directly related to the amplitude of the ITC binding curve; thus, ΔS_{el} can be obtained from eq 8:

$$\Delta S = \frac{\Delta H - \Delta G}{T} \quad (8)$$

The Manning model based on the theory of counterion condensation has certain constraints, such as the assumption of straight line charge spacing.[10,29] In addition, other factors such as electrostatic force, hydration or dehydration, hydrogen-bonding, and conformational change are not considered in the model. For HASE polymers in aqueous solution, l_B is 7.1 Å and the calculated values of m are 0.75, 0.67, 0.56, and 0.42 for HASE70−30, HASE60−40, HASE40−60, and HASE30−70, respectively.[10,29] The enthalpy (ΔH_{el}) and entropy (ΔS_{el}) of the electrostatic binding for HASE series polymers in 0.1 M NaCl solutions are summarized in Table 1. The entropy appears to be independent of MAA/EA molar ratios and remains essentially constant at 44 J/(mol K).

The second and third peaks corresponding to the formation of polymer-bound micelles and free micelles, respectively, can be quantified and parametrized by applying the semiquantitative approach based on the pseudo-phase separation model. The model assumes that the micelles exist as a separate microphase in equilibrium with the solution containing solvent and free surfactant and the composition of the phases are independent of the phase volumes.[10,12,14,15,19,30] The Gibbs energy of micellization, ΔG_{mic}, derived from the pseudo-phase separation model is given by

$$\Delta G_{mic} = (K + 1)RT \ln(\text{cmc}) \quad (9)$$

where K is the effective micellar charge fraction with a value of 0.77 for DoTab.[19,30] Free energy, enthalpy, and entropy corresponding to the micellization of electrostatic-bound surfactant (designated as $\Delta G'$, $\Delta H'$, and $\Delta S'$, respectively) and formation of free micelles (designated as ΔG_m, ΔH_m, and ΔS_m, respectively) are summarized in Table 1. As suggested by the thermodynamic parameters listed in Table 1, the formation of polymer-bound and free micelles are driven by entropy gain, which is related to the disruption of solvent cage due to micellization. It is noted that $\Delta S'$ is higher than ΔS_m, which is attributed to the different status of counterion condensation on the surface of polymer-bound and free micelle. For free ionic micelle, counterions are condensed on its surface and lose their translational entropy, which is thermodynamically unfavorable for the micellization and accounts for the higher cmc of ionic surfactants compared with nonionic ones. However, the surface of polymer-bound micelle is stabilized by the oppositely charged polymer chains; thus, counterions are not condensed on the micelle surface, and their translational entropy is preserved. Therefore, the micellization is enhanced as demonstrated by a smaller C' compared to C_m, and $\Delta G'$ is more negative than ΔG_m. We believe that the entropy corresponding to the formation of polymer-bound micelles (i.e., $\Delta S'$) is attributed purely to the release of water molecules expelled from the "solvent cage". On the other hand, entropy corresponding to the formation of free micelles (ΔS_m) consists of a negative entropy loss from condensed counterions (designated as ΔS_{cc}), which is given by the difference between ΔS_m and $\Delta S'$:

$$\Delta S_{cc} = \Delta S_m - \Delta S' \quad (10)$$

The translational entropy loss from counterion condensation was determined to be approximately 30 J/(mol K).

Effect of Salt on the Binding Characteristics. Figure 12 depicts the differential enthalpy curves of titrating 0.1 M DoTab solution into 0.05 wt % HASE70−30 solution with different NaCl concentrations. The addition of salt alters the electrostatic interactions between the macroions, counterions, and solvent molecules and significantly impacts the binding and micellization behaviors of DoTab surfactant. The enthalpy corresponding to the electrostatic interaction decreases from 13.24 to 5.65 kJ/mol when the NaCl concentration increases from 0.01 to 0.3 M (see Table 3). The addition of neutral salt suppresses the electrostatic attraction between the negative carboxylate groups and positive DoTab molecules; hence, the heat effect from the electrostatic interaction is less pronounced, and the amplitude of enthalpy peak decreases with increasing NaCl concentrations. However, when the salt concentration is sufficiently low (e.g.,

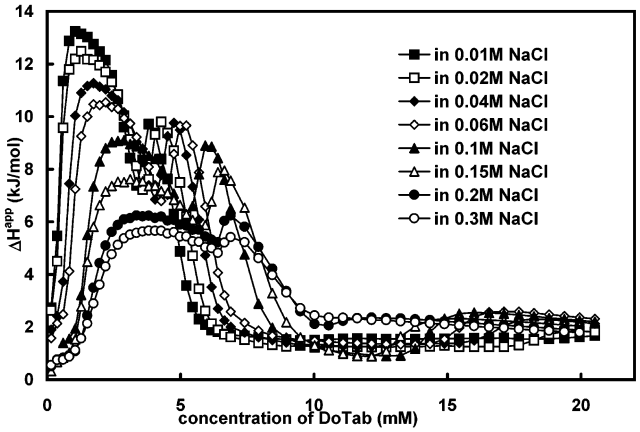

Figure 12. Differential enthalpy curves of titrating 0.1 M DoTab into 0.05 wt % HASE70−30 solutions with various NaCl concentrations: (■) 0.01 M; (□) 0.02 M; (◆) 0.04 M; (◇) 0.06 M; (▲) 0.1 M; (△) 0.15 M; (●) 0.23 M; (○) 0.3 M.

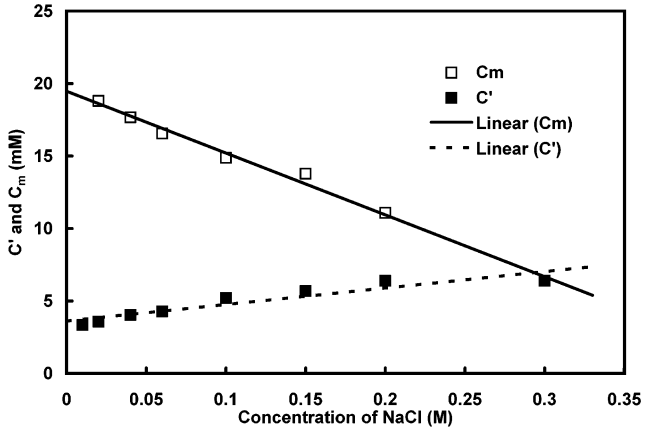

Figure 13. Dependence of C' and C_m NaCl concentration: (□) C_m; (■) C'.

TABLE 2: Critical Concentrations Obtained from Binding Isotherms at Different NaCl Concentrations for HASE/DoTab System

concn of NaCl (M)	C_1 (mM)	C' (mM)	C_2 (mM)	C_m (mM)
0.01	<0.14	3.34	5.92	>20
0.02	<0.14	3.58	6.16	18.81
0.04	0.37	4.04	6.63	17.67
0.06	0.60	4.28	6.90	16.55
0.1	0.83	5.21	8.43	14.88
0.015	0.94	5.69	9.49	13.79
0.2	1.05	6.40	10.01	11.08
0.3	1.05	6.40	10.01	6.40

less than 0.1 M), the addition of salt has negligible effect on the enthalpy for the polymer-induced micellization process indicated by the second peak (Figure 12).

The critical concentrations derived from the enthalpy curves at different salt concentrations are summarized in Table 2. It is noticed that C_1 shifts to higher value and the width of the first peak increases with increasing salt concentrations. The addition of salt screens the electrostatic attraction between the polymer/surfactant pair via an ionic atmosphere around the charged sites on the polymer chains. Thus more DoTab molecules are required to neutralize the screening effect of the ionic atmosphere before the onset of binding. These observations are attributed to two processes: (i) the cancellation of the screening effects introduced by the addition of salt and (ii) polymer/surfactant electrostatic interactions. We note that C', which characterizes the micellization of electrostatic-bound surfactant, shifts to higher values with increasing NaCl concentrations. As suggested by the ITC enthalpic curves, the micellization is electrostatically induced and occurs when the carboxylate sites are fully saturated with bound surfactant molecules.[10] The addition of salt hinders the polymer/surfactant electrostatic attraction, which suppresses the micellization and hence delays its occurrence. On the other hand, C_m, which corresponds to the formation of free micelles, decreases with NaCl concentrations.

We observe that both C' and C_m exhibit a linear relationship with the NaCl concentration as shown in Figure 13. Obviously, the addition of salt is detrimental to micellization of electrostatically bound surfactants, but it enhances the formation of free micelles. As predicted by Figure 13, C' and C_m intersect when NaCl concentration reaches approximately 0.3 M. This means that the electrostatic attractive force between polymer and surfactant and the repulsive force between surfactant molecules are greatly suppressed at very high salt concentration at which C' and C_m approach the same value and the polymer-bound and free micelles form simultaneously. This is consistent with the results obtained from our previous study on the binding and micellization behavior in the PAA/DoTab system.[10]

The thermodynamic parameters at various salt concentrations are summarized in Table 3. Several observations can be deduced from the data: (1) Addition of salt alters the enthalpy, entropy, and free energy for the electrostatic binding. The negative free energy ($-\Delta G_{el}$) decreases with increasing salt concentration, indicating that binding is unfavorable with the addition of salt because of charge-shielding effect, which weakens the electrostatic attractive force between the polymer/surfactant pair. The entropy (ΔS_{el}), which is attributed to the recovery of translational entropy of released counterions, decreases from 73.2 to 26.5 J/(mol K) as the NaCl concentration increases from 0.01 to 0.3 M. It may suggest that counterions condensed on the polymer chains cannot be fully released because of the considerably weaker binding and relatively stronger condensation at high salt condition. (2) The negative free energy ($-\Delta G'$) and entropy ($\Delta S'$) corresponding to the micellization of polymer-bound surfactant decrease from 25.0 to 22.2 kJ/mol and from 116.5 to 92.5 J/(mol K), respectively, when NaCl concentration is increased from 0.01 to 0.3 M, indicating that the polymer-

TABLE 3: Thermodynamic Parameters Derived from ITC of 0.1 M DoTab into 0.05 wt % HASE70−30 at Different Salt Concentrations

concn of NaCl (M)	ΔH_{el} (kJ/mol)	ΔS_{el} (J/(mol K))	ΔG_{el} (kJ/mol)	$\Delta H'$ (kJ/mol)	$\Delta S'$ (J/(mol K))	$\Delta G'$ (kJ/mol)	ΔH_m (kJ/mol)	ΔS_m (J/(mol K))	ΔG_m (kJ/mol)
0.01	13.24	73.2	−8.56	9.71	116.5	−25.00			
0.02	12.48	66.3	−7.27	9.80	115.8	−24.70	1.82	64.6	−17.43
0.04	11.27	57.9	−5.98	9.76	113.9	−24.17	2.25	66.9	−17.70
0.06	10.54	52.9	−5.23	9.66	112.7	−23.92	2.39	68.9	−18.13
0.10	9.07	44.8	−4.28	8.90	107.2	−23.05	2.50	70.3	−18.45
0.15	7.62	37.4	−3.53	7.95	102.8	−22.67	2.31	70.8	−18.79
0.20	6.23	30.9	−2.99	6.24	95.3	−22.15	2.33	74.1	−19.75
0.30	5.65	26.5	−2.24	5.42	92.5	−22.15			−22.15

induced micellization is unfavorable in the presence of salt. Because this process is induced by electrostatically bound DoTab surfactant molecules, addition of salt weakens the binding. (3) The negative free energy ($-\Delta G_m$) and entropy (ΔS_m) corresponding to the formation of free micelles increase from 17.4 to 19.8 kJ/mol and from 64.6 to 74.1 J/(mol K), respectively, as the NaCl concentration increases from 0.02 to 0.2 M. This suggests that the formation of free micelles is favored in the presence of salt and the electrostatic repulsive force between the surfactant headgroups is screened.

Conclusion

The HASE/DoTab system exhibits two peaks in the enthalpy curves. The first peak characterizes the electrostatic binding of cationic surfactant headgroups to the anionic sites on the polymer chains; the second peak corresponds to the micellization of polymer-bound surfactant molecules at a critical surfactant concentration (denoted as C'). Thermodynamic parameters extracted from ITC curves suggest that both the electrostatic binding and micellization are enthalpy-opposed and driven by entropy. The positive entropy for the electrostatic binding is attributed to the recovery of translational entropy of released counterions by the bound surfactant, whereas the entropy gain for micellization is attributed to the disruption of water structure.

The light scattering studies on the HASE/DoTab system show that both R_h and R_g increase by several times and the polymer solution precipitates at C', characterizing the formation of HASE/DoTab complex produced by the micellization of polymer-bound surfactants. Additional DoTab reduces the particle size of the complex, which is attributed to the reorganization of the polymer-bound micelle structure from cylindrical to spherical micelles. Thereafter the complex is either resolublized (for HASE polymer with low MAA composition) or gelatinized (for HASE polymer with high MAA composition) with further addition of DoTab.

The presence of a neutral salt screens the electrostatic attraction between the polymer/surfactant pair, which delays the onset of electrostatic binding. Addition of salt suppresses the micellization of polymer-bound surfactant but favors the formation of free micelles in solution. As predicted by the ITC binding profiles, the electrostatic attraction between polymer/surfactant pair is completely screened and the binding is totally suppressed for salt concentration greater than 0.3 M.

References and Notes

(1) Anthony, O.; Zana, R. *Langmuir* **1996**, *12*, 1967.
(2) Ghoreishi, S. M.; Fox, G. A.; Bloor, D. M.; Holzwarth, J. F.; Wyn-Jones, E. *Langmuir* **1999**, *15*, 5474.
(3) Li, Y.; Ghoreishi, S. M.; Warr, J.; Bloor, D. M.; Holzwarth, J. F.; Wyn-Jones, E. *Langmuir* **1999**, *15*, 6326.
(4) Merta, J.; Stenius, P. *Colloids Surf. A* **1999**, *149*, 367.
(5) Konop, A. J.; Colly, R. H. *Langmuir* **1999**, *15*, 58.
(6) Khokhlov, A. R.; Dormidontova, E. E. *Physics-Uspekhi* **1997**, *40* (2), 109.
(7) Ghoreishi, S. M.; Li, Y.; Holzwarth, J. F.; Khoshdel, E.; Warr, J.; Bloor, D. M.; Wyn-Jones, E. *Langmuir* **1999**, *15*, 1938.
(8) Ehtezazi, T.; Govender, T.; Stolink, S. *Pharm. Res.* **2000**, *17*, 871.
(9) Matulis, D.; Rouzina, L.; Bloomfield, V. A. *J. Mol. Biol.* **2000**, *296*, 1053.
(10) Wang, C.; Tam, K. C. *Langmuir* **2002**, *18*, 6484.
(11) Fundin, J.; Hansson, P.; Brown, W.; Lidegran, I. *Macromolecules* **1997**, *30*, 1118.
(12) Goddard, E. D. In *Interactions of Surfactants with Polymers and Proteins*; Goddard, E. D., Ananthapadmanabhan, K. P., Eds.; CRC Press: Boca Raton, FL, 1993; pp 171.
(13) Evertsson, H.; Holmberg, C. *Colloid Polym. Sci*. **1997**, *275*, 830.
(14) Seng, W. P.; Tam, K. C.; Jenkins, R. D.; Bassett, D. R. *Macromolecules* **2000**, *33*, 1727.
(15) Seng, W. P.; Tam, K. C.; Jenkins, R. D.; Bassett, D. R. *Langmuir* **2000**, *16*, 2151.
(16) Wang, G. Ph.D. Thesis, Lund University, Lund, Sweden, 1997.
(17) Olofsson, G.; Wang, G. *Pure Appl. Chem.* **1994**, *66*, 527.
(18) Wang, G.; Olofsson, G. *J. Phys. Chem.* **1995**, *99*, 5588.
(19) Wang, Y.; Han, B.; Yan, H.; Kwak, J. C. T. *Langmuir* **1997**, *13*, 3119.
(20) Fox, G. J.; Bloor, D. M.; Holzwarth, J. F.; Wyn-Jones, E. *Langmuir* **1998**, *14*, 1026.
(21) Shirahama, K. The Nature of Polymer−Surfactant Interactions. In *Polymer−Surfactant Systems*; Kwak, J. C. T., Ed.; Marcel Dekker, Inc.: New York, 1998.
(22) Rodenhiser, A. P.; Kwak, J. C. T. Polymer−Surfactant Systems: Introduction and Overview. In *Polymer−Surfactant Systems*; Kwak, J. C. T., Ed.; Marcel Dekker, Inc.: New York, 1998.
(23) Islam, M. F.; Jenkins, R. D.; Bassett, D. R.; Lau, W.; Ou-Yang, H. D. *Macromolecules* **2000**, *33*, 2480.
(24) Dai, S.; Tam, K. C.; Jenkins, R. D. *Eur. Polym. J.* **2000**, *36*, 2671.
(25) Wiseman, T.; Williston, S.; Brandts, J. F.; Lin, L. *Anal. Biochem.* **1989**, *179*, 131.
(26) Jelesarov, I.; Bosshard, H. R. *J. Mol. Recognit.* **1999**, *12*, 3.
(27) Wang, C.; Tam, K. C.; Jenkins, R. D.; Bassett, D. R. *Phys. Chem. Chem. Phys.* **2000**, *2*, 1967.
(28) Manning, G. S. *J. Chem. Phys.* **1969**, *51*, 924.
(29) Lindman, B.; Thalberg, K. In *Interactions of Surfactants with Polymers and Proteins*; Goddard, E. D., Ananthapadamananabham, K. P., Eds; CRC Press: Boca Raton, FL, 1993; p 203.
(30) Linse, P.; Piculell, L.; Hansson, P. In *Polymer−Surfactant Systems*; Kwak, J. C. T., Ed.; Marcel Dekker: New York, 1998; p 193.